ChemSusChem

Chemistry Europe
European Chemical Societies Publishing
ChemSusChem

RESEARCH ARTICLE

Cascade Valorization of Brewer's Spent Grain Residues Through Green Solvent Extractions and Subsequent Thermochemical Conversion to Activated Carbon Adsorbers

Dries Bleus[1,2] | Nahal Ghanemnia[1,2] | Wouter Marchal[1,2] | Dries Vandamme[1,2]

[1]Analytical and Circular Chemistry (ACC), Institute for Materials Research (IUMAT), UHasselt, Hasselt, Belgium | [2]imec, IUMAT, Diepenbeek, Belgium

Correspondence: Wouter Marchal (wouter.marchal@uhasselt.be)

Received: 13 January 2026 | **Revised:** 7 July 2026 | **Accepted:** 30 July 2026

Keywords: activated carbon | adsorption | biorefinery | chemistry | pyrolysis | solvent extraction

ABSTRACT

To maximize the recovery of multiple added-value products from biomass waste streams, optimal valorization should follow a cascade process integrating extraction and conversion steps. In this context, natural deep eutectic solvents (NADES) can be employed as green solvents to significantly expand the possible valorization routes. In this study, brewer's spent grain (BSG) was first used for antioxidant (polyphenolic compound) extraction with NADES, whereupon the remaining biomass was converted into activated carbons (ACs). These adsorbents were characterized in-depth, and their performance for subsequent NADES clean-up is described for the first time as a proof-of-concept. Extraction with NADES caused a significant reduction in AC yield, due to associated degradation effects on structural elements (lignin, cellulose, and hemicellulose) within the biomass. The largest effect (only 3% AC yield for choline chloride:malic acid) was correlated to the solvent acidity, and not inherent to the NADES hydrogen bond interactions. In addition, the acidic pretreatment caused significantly lower surface area and less micropore development, which negatively impacted the adsorption properties. Nonetheless, NADES pretreatments created ACs that outperform traditional woody-biomass-derived commercial AC reference materials (adsorption q_e of 203.9 ± 12.5, 257.3 ± 6.8, and 204.9 ± 2.8 mg/g, respectively, from choline chloride:glycerol NADES stock solution).

1 | Introduction

Sustainable food production stands as one of the defining global challenges of the 21st century, with increasing population growth, resource scarcity, and environmental degradation necessitating a fundamental shift in how food systems operate [1]. As part of this transition, there has been an intensified research focus on circular economy strategies, particularly on waste-to-food and waste-to-chemicals valorization pathways [2–8].

However, a broad vision is required for valorizing biomass waste streams in an efficient, cost-effective, and, most importantly, environmentally net-positive way [9, 10]. An aspect of biomass reuse that is often overlooked is the fact that many of the proposed techniques only reuse a small fraction of the resource and hence produce a subsequent waste stream of their own. By combining synergistic state-of-the-art valorization processes, a global cascade methodology with a more complete utilization of the available biomass can be obtained. This not only creates more value-added products, but also helps minimize process costs and environmental burden. Especially the latter, economic and environmental cost, is difficult to quantify, and depends on the methodology but also external elements such as the avoided transportation by combining two or more processes, the reuse of residual heat within the

own cycle, and optimized plant construction requiring less equipment and energy to achieve similar goals [11, 12].

Hence, cascade valorization frameworks are increasingly being reported in literature, with a particular focus on lignin refineries and bioenergy applications [13–16]. For instance, Wu et al. investigated cascade lignin extraction followed by enzymatic saccharification of the remaining cellulosic fraction to obtain glucan [17]. Cascade approaches are also commonly employed for the production of bioethanol or biogas [13, 18]. For example: Rabelo et al. presented a cascade pathway to obtain lignin-derived products as well as bioethanol, through enzymatic hydrolysis and fermentation of the rest fractions [18].

But valorization pathways can also target more high-value bioactive compounds and specialty chemicals, such as phenolic compounds (PC). PC extraction from biomass residues, using green solvents such as natural deep eutectic solvents (NADES), has gained significant attention in the state-of-the-art [19–24]. The production of biochar or subsequent activation to form activated carbons (ACs) has been illustrated before as a suitable work-up method to deal with nonsoluble rest fractions obtained from extraction. As demonstrated by Zabaniotou et al., pyrolysis offers a practical methodology to convert nonsoluble fractions into high-value functional materials and provides a good total mass yield of the biomass stream [25].

By integrating NADES extraction pretreatment together with downstream thermochemical conversion, this study contributes to the underexplored development of closed-loop biomass valorization frameworks using green solvents and offers new insights into the synergistic potential of cascade biorefinery processes. As mentioned above, green-solvent pretreatments can have extensive effects on lignocellulosic biomass streams [15]. This work particularly explores these effects of structurally and compositionally altered spent biomass residues by NADES extraction "pretreatment," on the production of biochars and subsequent ACs.

The first stage, recovery of phenolic compounds (PC) from BSG through high-temperature extraction with NADES, has been the topic of previously published work [26]. PCs offer extensive application potential in various industries, ranging from food and feed additives or nutraceuticals, to pharmaceuticals or advanced materials [27–31]. This manuscript focuses on the spent BSG residue that has been structurally and compositionally altered by the upstream high-temperature, NADES-assisted hydrothermal, extractions (using choline chloride:glycerol in a 1:2 molar ratio (ChCl:Gly) and choline chloride:malic acid in a 1:1 molar ratio (ChCl:Ma)) and compares them against untreated "virgin" BSG, and pretreatments methods with more traditional solvents, such as hydrothermal treatment with pure water, and water with mild acidic properties (using low percentages of malic acid), so as to get a better understanding how pretreatment with NADES differs from classic solvents. The choice of different green extraction solvents is observed to have far-reaching consequences for the structural composition of the biomass, dictating for a large part the further usability, mass balance, and functionality of the biomass stream in a cascading step [26, 32].

A secondary valorization of said spent biomass is performed through pyrolysis and mild CO_2-assisted physical activation to form AC, or bio-based adsorbers (BBA). For the first time, the influence of the preceding extraction step on the pyrolysis and activation behavior of the spent biomass is critically assessed through in-depth characterization of the biomass and subsequent ACs.

Bio-based ACs are currently under extensive investigation for their use as separation media, particularly in the field of inorganic (heavy metals) or organic (e.g., organic dyes or polyaromatic hydrocarbons) polluents [33–36]. Thus, as a final step in this work, a closed-loop circular process is obtained by utilizing the produced ACs as a novel separating agent in the process of purifying green-solvent extracts obtained from the preceding cascade valorization step. This is of particular interest for both obtaining pure PC extracts, and recycling the extraction solvent, as NADES are particularly difficult to recycle through conventional techniques due to their low vapor pressure [37].

Proof-of-concept for this novel application is obtained by means of a kinetic study on model PC extractions from different NADES solvents, using BBA. This also highlights the differences in obtained physicochemical material properties of the pretreated ACs and the impact on adsorption properties. Finally, a novel desorption strategy is discussed to recover PC from the AC's in a final stage, thus closing the loop of the proposed circular methodology. This proof-of-concept for the use of BBA as separation media could provide a stepping stone toward successful application of green solvents (such as NADES) in large-scale industrial extraction and biomass valorization processes.

2 | Materials and Methods

2.1 | Chemicals and Reagents

BSG biomass was obtained from Alken-Maes brewery (Alken, Belgium) and immediately dried at 65 °C until the residual water content was approximately at or below 5 wt%. Malic acid, glycerol, and choline chloride, used to prepare NADES formulations, were obtained from Thermo Fischer Scientific, (Waltham, USA). For the high-performance liquid chromatography (HPLC) analysis, ferulic acid (FER; Thermo Scientific, Waltham, USA), caffeic acid (CAFF; Thermo Scientific, Waltham, USA), p-coumaric acid (COUM; Thermo Scientific, Waltham, USA), and syringaldehyde (SYR; TCI chemicals, Tokyo, Japan) were used as standards for prevalent phenolic compounds. LC-grade Formic acid (LiChropur; Merck, Darmstadt, Germany) was used to acidify the samples for HPLC analysis. Analytical reagent grade acetone (AnalaR NORMAPUR) and analytical reagent grade Methanol (HiPerSolv CHROMANORM for LC-MS) were obtained from VWR (Radnor, USA). Ultrapure (UP) water (18 MΩ*cm) was obtained using an Arium Pro System (Sartorius, Göttingen, Germany), fresh UP water was prepared every day to prevent impurities.

2.2 | Extraction "Pretreatment"

BSG samples were extracted using a hydrothermal method (HTE) at 120 °C, for 60′. The extraction was performed with each of the following solvents: ultrapure (UP) water ("H_2O"), malic acid:UP water (5 wt% malic acid; "Ma:H_2O"), malic acid:choline chloride

NADES (1:1 molar ratio, 25 wt% H2O; "ChCl:Ma"), and glycerol: choline chloride NADES (2:1 molar ratio, 25 wt% H_2O; "ChCl:Gly"). Extracts were separated using vacuum filtration, and the remaining solid biomass residue was washed with UP water, before drying at 105 °C to remove moisture. All extractions were performed in duplo, except for the benchmark sample "H_2O." Duplicate samples were further processed as mixed samples to minimize effects of batch-to-batch variation.

2.3 | Preparation of AC

Figure 1B shows the home-built pyrolysis reactor manufactured in stainless steel (AISI 304), which was developed for batch pyrolysis and steam or gas activation of biomass samples on a small scale (<40 g). A ceramic crucible inside the furnace was used to hold the relatively small quantities of (extracted) BSG sample used in this experiment and ensure homogenous heat transfer throughout the sample. The reactor was heated using a furnace (Nabertherm) controlled by a programmed FGH 1000 controller with a *K*-type thermocouple feedback loop to control the heating cycle based on internal temperatures of the reaction chamber.

For pyrolysis, 8.000 g (±0.030 g) of sample was weighed in a ceramic crucible and heated under N_2 atmosphere (70 ml/min) according to the following temperature program (Figure 1A): RT – 700 °C (15 °C/min ramp), isothermal at 700 °C (30′), cooldown. Biochar samples were collected after pyrolysis, weighed, and crushed to a homogenous particle size < 0.5 mm. Pyrolysis experiments were carried out once for all but samples "UNTR" and "Ma:H_2O," which were performed in duplo to evaluate repeatability of the experiment.

For activation, 800 mg (±10 mg) of biochar was weighed in a ceramic crucible and spread out evenly to ensure homogenous contact with activating agent. The sample was heated under N_2 atmosphere according to the following program: heated under N_2 atmosphere according to the following program: RT – 15 °C/min ramp – 700 °C, IsoT 700 °C (30′), 700 °C – 15 °C/min ramp - 900 °C*, IsoT 900 °C (30′) under CO_2 atmosphere, cooldown. A 10:1 mass ratio of CO_2:Biochar was enabled by setting a controlled CO_2 gas flow of 133 ml/min. All activation experiments were performed in duplo.

2.4 | Activated Carbon Post-Treatment

All AC materials were washed with a 1 M HCl solution 10:1 washing liquid:AC ratio and stirred at 40 °C for 1 h. The AC samples were then filtered off and rinsed with UP water until a neutral pH of the washing liquid was obtained. The washed AC samples were dried at 105 °C, and final solid weight was recorded. The mass loss due to post-treatment is further referred to as acid-soluble ash (ASA) content.

2.5 | Ultimate Analysis

Elemental composition (carbon, hydrogen, nitrogen, and sulfur content) of all AC samples was recorded after HCl posttreatment, using a Thermo Electron Flash EA1112 elemental analyzer (Thermo Fischer Scientific, Waltham, USA). The instrument was calibrated with a reference standard: BBOT (2,5-bis (5-tert-butyl-benzoxazole-2-yl) thiophene) (Thermo Fischer Scientific, Waltham, USA). For each analysis, between 3 and 4 mg of sample was weighed. All samples were measured in quadruplicate.

2.6 | Gravimetric Ash Content

Due to the small-scale production of ACs, ash content was determined based on the relative mass loss between 105 and 650 °C observed in a thermogravimetric analysis performed on a TA instruments Q500 apparatus (TA instruments, New Castle, USA).

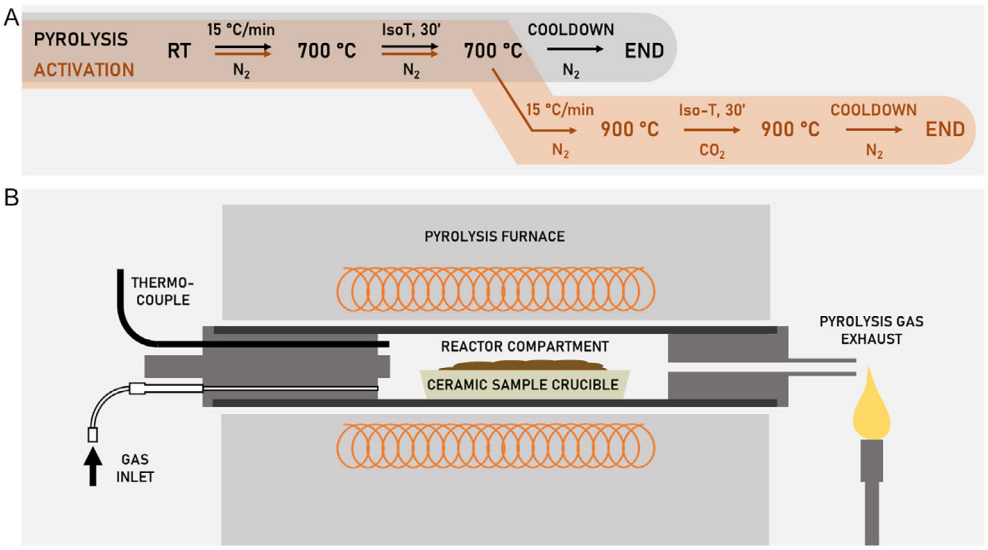

FIGURE 1 | (A) Overview of the pyrolysis (gray) and activation (orange) sequence parameters; (B) schematic depiction of the custom-built pyrolysis setup using a 316 L stainless steel pipe pyrolysis chamber in a Nabertherm furnace.

Samples of approximately 5 mg were heated under atmospheric conditions (heating rate 20 °C/min).

2.7 | Gas Physisorption

The AC surface properties were analyzed via N_2/CO_2 physisorption at 77 K with a Tristar II 3020 surface area analyzer (Micromeritics, Norcross, USA). Prior to the measurements, the samples were degassed under nitrogen flow at 150 °C for 16 h. The specific surface area (S_{BET}) was calculated via the Brunauer–Emmett–Teller theory. Pore size distribution (PSD) was determined based on a combined N_2 and CO_2 NLDFT fitting.

2.8 | Inorganic Content Composition

Inorganic elemental composition was determined using inductively coupled plasma–optical emission spectroscopy (ICP–OES) on an Optima 3000 DV ICP-OES instrument (PerkinElmer, Waltham, USA) in axial viewing mode. Instrument calibration was done using ICP Merck multistandard solution IV. The main elements of interest were Ca, K, Mg, Fe, Al, alongside elements which were present in lower concentrations, such as Na, Ni, Pb, Sr, Zr, Mn, Cr, Ba (designated as "other").

2.9 | (Kinetic) Adsorption Test

For each AC sample, 15 mg AC was weighed in a closed vial. Samples were prepared in duplicate. To each sample, 6 ml of 250 ppm PC stock solution in NADES (ChCl:Gly or ChCl:Ma) was added. Samples were stirred at RT for 24 h, with sampling at 0.5, 1, 3, and 24 h. For each sampling, one milliliter was removed from the sample, and filtered on a 0.45 mixed cellulose ester syringe filter to remove the AC and stop adsorption. All samples were further diluted 1:1 with acidified UP water (2% formic acid) before HPLC analysis. Concentrations were calculated based on an external calibration curve with standard mix samples between 0 and 250 ppm of caffeic acid (CAF), syringaldehyde (SYR), p-coumaric acid (COUM), and ferulic acid (FER).

The percentage of PC adsorption was calculated using Equation (1):

$$\text{Relative adsorption (rel. \%)} = (C_0 - C_e)/C_0 * 100 \quad (1)$$

where C_0 (mg L^{-1}) and C_e (mg L^{-1}) are the initial and equilibrium concentrations of CAF, SYR, COUM, and FER, respectively.

Kinetic adsorption rates were determined based on a pseudosecond-order fitting (Equation (2)) using a damped least-squares (DLS) curve fitting. All curves were checked for fit based on low residual mean square and suitably high R^2 (>0.99) values.

$$q_t = \frac{{q_e}^2 * k_2 * t}{1 + q_t * k_2 * t} \quad (2)$$

where q_t: amount of adsorbate adsorbed at time t; q_e: amount of adsorbate adsorbed at equilibrium; k_2: pseudosecond-order rate constant.

3 | Results and Discussion

3.1 | Conversion Yields of ACs Obtained From Extraction Pretreated Versus Virgin Biomass

The most prominent effect of extraction pretreatment is the removal of solid material from the biomass matrix, creating mass transport of the targeted polyphenolics to the respective solvent. The choice of solvent and extraction conditions can also remove other soluble side products and, in some cases, can cause structural changes within the biomass (through degradation of structural elements and larger macromolecules) [38]. Due to the strong influence of the extraction medium and conditions on structural components such as hemicellulose and lignin, hydrothermal extraction pretreatment—especially due to the high process temperatures—is expected to have a significant effect on pyrolysis yield outcomes [39–42]. This is apparent in the solids conversion yields after extraction (Figure 2), which are drastically reduced for the more aggressive treatments with aqueous malic acid (Ma:H_2O) and ChCl:Ma NADES (53% and 45%, respectively). More benign extraction solvents, such as pure water and ChCl:Gly NADES, show distinctly higher conversion yield during the extraction stage, 83% and 91%, respectively. Hence, it can be expected that the extracts obtained from acid media will also contain a larger amount of untargeted side products, which would have to be removed from the extract to obtain pure PC.

The impact of solid material removal during extraction translates into reduced AC yields after thermochemical conversion, as opposed to the AC obtained from the unextracted BSG residue. Instinctively, one would expect that yield changes mostly arise due to the disruption and removal of volatile, labile, and free small-molecule compounds, which would otherwise be removed during the pyrolysis process. The sample pretreated with only ultrapure (UP) water ("H_2O") shows a slightly reduced conversion yield (10.0 ± 0.3%) compared to the untreated sample (11.4 ± 0.2%), highlighting that the structural changes are not merely an effect of the high pretreatment temperature (hydrothermal extraction at 120 °C), but rather water is a benign solvent that does not significantly impact the material. This is in line with pyrolysis pretreatment studies done by Diao et al. [43].

In contrast, the combined pyrolysis and activation conversion yields for acid pretreated samples Ma:H_2O and ChCl:Ma, are drastically reduced (2.4 ± 1.3% and 3.0 ± 0.8%, respectively). The removal of hemicellulosic structures, and potentially also an influence on lignin, is thus confirmed to have an adverse effect on pyrolytic recalcitrance [44]. As observed in previous work, ChCl:Gly NADES is an effective extraction medium in HTE-assisted extraction, though it results in overall less aggressive treatment conditions, and thus less pretreatment induced structural changes are expected. In that sense, the observed pyrolysis yield aligns well with the expected effect of the pretreatment, yielding a mass conversion of 7.3 ± 0.2%.

3.2 | Impact of Extraction Pretreatment on AC Surface Area

In the previous section, the influence of acidic extraction media on pyrolysis and activation conversion yields was illustrated.

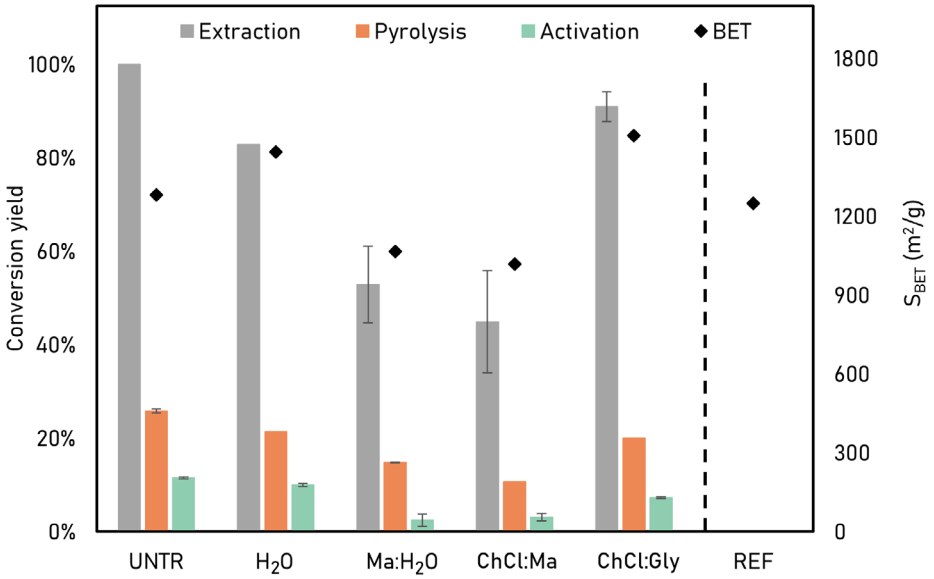

FIGURE 2 | Total solids conversion yield after each treatment step (hydrothermal extraction, pyrolysis, CO_2 activation) expressed as relative percentage to the initial dry weight (DW) of the BSG biomass (left *y*-axis). Note that the UNTR sample was unextracted, thus the extraction yield represents 100% of the initial DW. Note that for the reference AC, no conversion yield is provided. Specific surface area (as calculated by BET theory based on N_2 gas physisorption isotherms) for the AC samples is represented by ◆ (right *y*-axis).

However, several mechanisms occur simultaneously, limitations to the activation process and how far this pore formation can be pushed. This becomes clear when comparing the effect of the different NADES pretreatments on BSG samples, which were all pyrolyzed and activated using a mild physical activation agent, CO_2, following the same procedure.

It is well-known that surface area development is closely linked to conversion, as the (physical or chemical) activation agent reacts with the carbonaceous matrix and gradually creates porosity. Hence, the slightly higher carbon burn-off observed for ChCl:Gly as opposed to UNTR or H_2O AC samples results in the highest BET specific surface area (S_{BET}) among all tested conditions (Figure 2). However, the extremely high carbon burn-off (low AC mass yield) of the acid pretreated samples ChCl:Ma and Ma:H_2O (total yield of only 4.5%–7% throughout the total pyrolysis + activation process) translated into BET surface areas which were found to be approximately 25% lower than both ChCl:Gly and H_2O pretreated ACs. For the acid-treated samples, once mass loss due to extraction is accounted for, the total AC yield is down to only 2.4% and 3.0% for Ma:H_2O and ChCl:Ma, respectively. Instinctively, one would expect these samples to create very strongly open networks due to the aggressive pretreatment of the biomass. It is, however, likely that the initial breakdown of recalcitrant material in the biomass due to the extraction in acidic media (Figure 2) causes a shift in the composition of the pretreated biomass toward relatively more labile and volatile content, which is later removed during pyrolysis. This is in line with studies by Zhang et al. and Tiryaki et al., which showed a significant impact of the presence of lignin and cellulose contents on increased (micro- and mesopore) surface area creation during activation [40, 45]. Thus, the breakdown of these structural components during pretreatment could lead to an adverse effect on pore formation.

Second, it must also be considered that activation is a destructive process that, in principle, can be performed until no more carbonaceous material is left. Initially formed pore sites are effectively eroded by continuous carbon burn-off causing pore wall collapse, as well as pore coalescence and sintering occurring at elevated activation temperatures. The combination of such effects translates into increasingly predominant meso- and macroporous structures in the AC [46–50]. Looking at Figure 3, which shows the carbonaceous versus inorganic ash composition of the final AC products, it is apparent that both acid-treated samples end up with a significantly lower carbonaceous content (only 0.8 and 1.7% of the initial biomass dry weight (DW), for Ma:H_2O and ChCl:Ma pretreated samples, respectively), and most microporous structures have likely been destroyed by the activation process. This is also confirmed by the PSD for these two materials (Figure S2), which shows a significantly lower microporous content, and for Ma:H_2O a significantly increased mesopore content. For these samples, an improved yield and porosity could potentially be attained with less intensive physical activation.

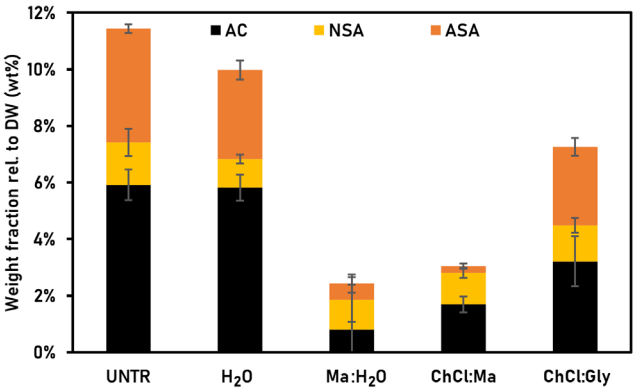

FIGURE 3 | Breakdown, in mass percentage, of AC total conversion yield into acid-soluble ash (ASA), nonsoluble ash (NSA), and the "actual" carbonaceous fraction remaining in the AC products obtained by different pretreatment (all values expressed as wt% relative to the initial dry weight (DW) of the initial BSG biomass; $\bar{x} \pm$ standard error (SE); $n = 2$).

3.3 | Impact of Pretreatment on Inorganic Content and Recalcitrant Matter in ACs

Inorganic ash content was expressed as a function of the total initial biomass mass after pretreatment, to visualize the differences obtained based on pretreatment method. Ash content was determined in two steps: the mass loss after acid washing of the obtained AC (acid-soluble ash; ASA) and the recalcitrant rest ash fraction obtained from TGA analysis of the acid-washed AC's (nonsoluble ash; NSA). Thus, the sum of both gives an idea of the ash or inorganic presence in the ACs right after pyrolysis.

Figure 3 shows a breakdown of the total AC conversion yield in carbonaceous matter, acid-soluble ash (ASA) and acid-insoluble ash (NSA), expressed as wt% relative to the initial biomass dry weight. The same data is also reported as full tabulated values in Table S2, providing a breakdown of the ash content into relative weight percentages of both the mass of AC material obtained after activation and of the total dry weight of the starting material.

It is clear that AC made from BSG extracted with an acid medium, such as aqueous malic acid, or ChCl:Ma NADES, has substantially less ash or inorganic content available for removal after activation (23.5 and 7.9 wt% ASA, respectively). It is interesting to note here that this drastic change was achieved by relatively weak organic acid (malic acid, pKa: 3.51). This indicates that most of this matter is either already removed in the extraction step or more strongly retained in the AC. Pure water, even using the same intense HTE method at 120 °C, does not yield a significantly different ash content from the untreated sample, and ChCl:Gly NADES-washed samples actually showed an inverse trend, with higher ash content in the remaining AC. ChCl:Gly does not possess the acidity required to wash out mineral fractions, but has a known effect on recalcitrant organic matter such as lignin [32, 51]. Hence, pretreatment with ChCl:Gly causes a relative higher inorganic matter content after AC, compared to fixed carbon.

A different side of the interpretation can be viewed as the removal percentage in function of the total mass of biomass that was converted to AC. Then, it can be observed even better that the two acidic media already removed a substantial amount of inorganic matter (approximately 3.4 and 3.8 wt% ASA removed, respectively, for Ma:H_2O and ChCl:Ma, relative to UNTR). The story of ChCl:Gly is somewhat more nuanced here; ChCl:Gly did

TABLE 1 | CHNSO and ash content (NSA) of the final ACs obtained through different extraction pretreatment pathways. Results obtained from combined data from CHNS and TGA analyses. Sulfur values were mostly below the detection limit of 0.5% (<DL).

	N	C	H	S	O	ASH (NSA)
UNTR	2.25 ± 0.20	72.20 ± 5.07	0.68 ± 0.04	<DL	4.69 ± 4.78	20.18 ± 6.48
H_2O	2.71 ± 0.10	80.27 ± 2.13	0.78 ± 0.11	<DL	1.50 ± 1.71	14.74 ± 2.09
Ma:H_2O	1.14 ± 0.10	39.98 ± 3.43	0.53 ± 0.06	0.89 ± 0.09	0.62 ± 0.33	57.29 ± 1.51
ChCl:Ma	2.13 ± 0.31	55.00 ± 2.70	0.58 ± 0.06	<DL	2.63 ± 2.37	39.66 ± 5.63
ChCl:Gly	1.90 ± 0.14	67.13 ± 4.60	0.65 ± 0.12	<DL	2.01 ± 7.01	28.32 ± 2.38
REF	0.42 ± 0.05	83.63 ± 0.69	0.00 ± 0.00	<DL	3.29 ± 0.00	12.67 ± 0.00

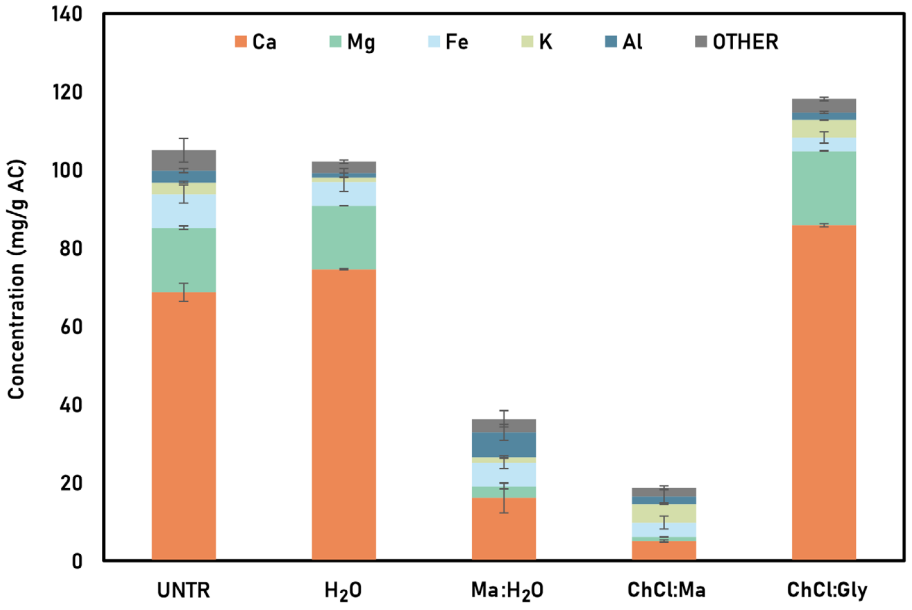

FIGURE 4 | ICP analysis of acid-soluble ash removed from AC during HCl washing post-treatment. (Results expressed as $\bar{x}$ ± standard error (SE); $n = 2$).

cause some removal of inorganic matter (roughly estimated, approximately. 1.2 wt% on BSG DW basis), more so than pure H_2O, but not to the degree of the two acidic solvents.

It can be observed that the total ash content of all pretreated samples is lower than that of the untreated AC, as expected. Interestingly, both acidic pretreatments (Ma:H_2O and ChCl:Ma) create an AC that still contains a substantial amount of inorganic matter, yet the majority is retained as NSA due to the pretreatment already removing most ASA or inorganic contents. The reduced recalcitrance of the pretreated biomass causes relatively much lower carbon content to remain in the final AC (Figure 3), with particularly low carbonaceous yields obtained for Ma:H_2O (2.4%), the final AC product obtained from that pretreated sample actually being composed of a majority of ash (67%) and only a minor fraction of actual carbonaceous matter (33%). Some of the ash is still removed during acid-washing (ASA), resulting in a final ash content of 57% (Table 1). ChCl:Ma pretreated AC also has a relatively high NSA content remaining in the final product (40%), both of which are significantly higher than the ash contents for UNTR, H_2O, and ChCl:Gly pretreated ACs, which have a final (NSA) ash content of 20%, 15%, and 28%, respectively. Besides weakening of the main structural biomass elements such as lignin and (hemi-)cellulose, the strongly reduced carbon retention for acid-pretreated samples can also be explained by the catalytic influence of inorganic mineral fractions on the creation of solid and gaseous pyrolysis products. As mineral content is reduced due to the acid washing, the balance is known to shift toward more pyrolysis oil production [44, 52, 53]. In this application, the effect of extensive mineral removal (with Ma:H_2O and ChCl:Ma pretreatments) was observed both in the pyrolysis and in the activation yield, creating an exaggerated reduction in yields. Similar effects were observed in demineralization studies by Vercruysse et al. on biochar as well as AC derived from

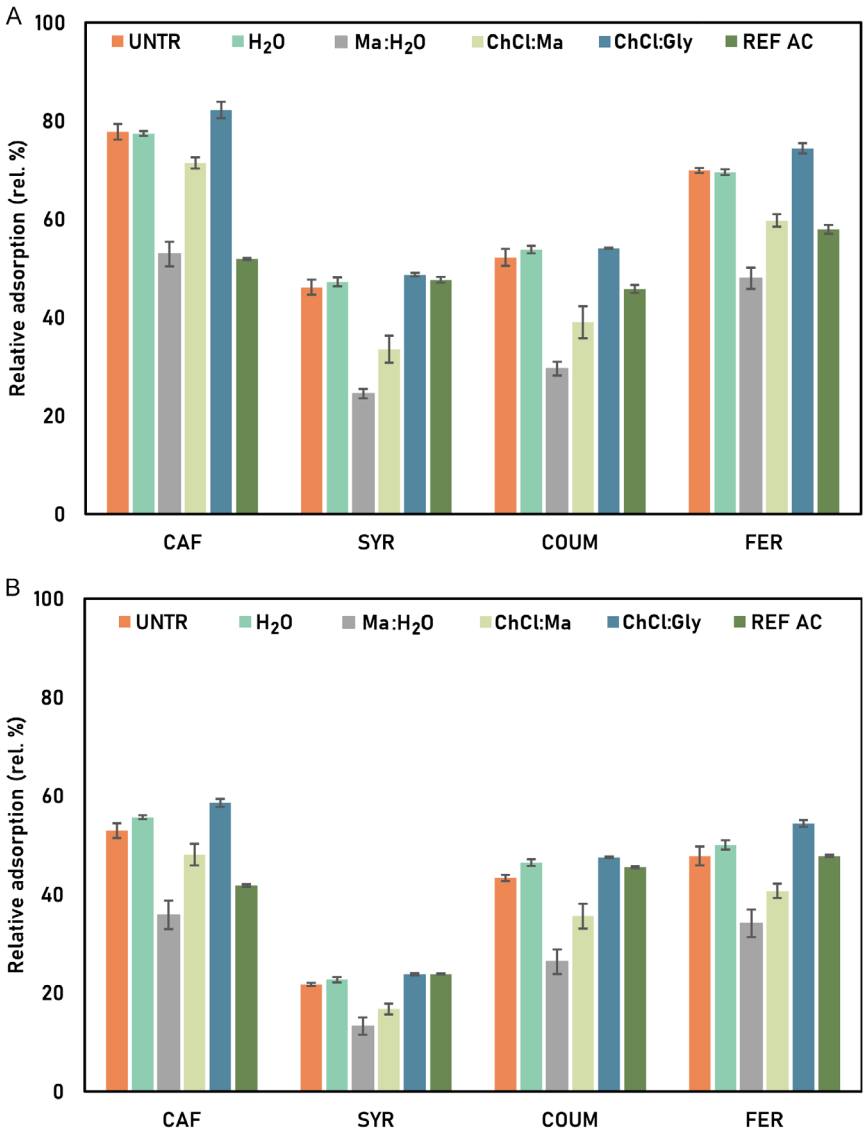

FIGURE 5 | Relative adsorption of the four individual phenolic compounds (caffeic acid (CAF), syringaldehyde (SYR), p-coumaric acid (COUM), and ferulic acid (FER)) using AC of: untreated BSG (UNTR); H_2O pretreated BSG (H_2O); aqueous malic acid pretreated BSG (Ma:H_2O); Ma:ChCl pretreated BSG (ChCl:Ma); Gly:ChCl NADES pretreated BSG (ChCl:Gly); Commercial reference AC (REF). Adsorption from a 250 ppm stock solution in: (A) gly:ChCl NADES (ChCl:Gly); (B) malic acid:ChCl NADES (ChCl:Ma). (Results expressed as $\bar{x} \pm$ standard error (SE); $n = 2$).

common Ivy [54]. Additionally, the high remaining ash content of ChCl:Ma and Ma:H_2O AC samples could also cause pore blockages, further reducing the final available surface area [49].

3.4 | Impact of Pretreatment on Compositional Changes of ACs

From the perspective of creating functional BBAs, a deeper analysis of the ACs composition can yield valuable information on how extractive pretreatment influences the formation of porous structures and surface functionality.

Despite high conversion of the acid-treated samples leading to a drastically lowered carbon content, the CHNSO analysis (Table 1) does not seem to indicate a similarly lowered nitrogen or oxygen content. The caveat here, preventing firm conclusions about the presence of heteroatoms (indicative of functional moieties through the respective N/C and O/C ratios), is that this analysis was not sensitive enough to provide accurate results at these low relative concentrations (as indicated by the high SE [Table 1]).

ICP analysis was performed on the inorganic mineral content in the ASA fraction, obtained during the HCl-wash postprocessing step, to obtain insights in the element-specific nature of the upstream pretreatment steps, and to try to identify the impact on adsorbent functionality (Figure 4). Acid washing is known to have a positive effect on the adsorbent functionality of AC, by eliminating some of the inorganic materials that remain chemically bound to the AC surface after pyrolysis [55, 56].

Based on the quantity of leachable compounds, it can be observed that a substantial amount of the inorganic material is removed during extraction with acidic media, while the effect of neutral media such as water or ChCl:Gly is negligible compared to the untreated reference. The presence of a major fraction of calcium plays a crucial role here, as calcium salts are generally poorly soluble in aqueous media and thus remain mostly present in the H_2O and ChCl:Gly pretreated samples. Malic acid-based extraction media Ma:H_2O and ChCl:Ma were proven highly effective at removal of alkaline earth metals (Ca and Mg).

The influence of this acid-soluble mineral fraction (ASA) on the formation of AC is has been studied literature, and it is generally accepted that (earth) alkali and metals such as K, Ca, Fe, and Mg play an important role in catalyzing the carbon conversion during CO_2 activation [57–59]. Thus, part of the explanation why the acid pretreated ACs Ma:H_2O and ChCl:Ma have less developed pore structures could be due to their much lower mineral content (as based on the amount of leachable inorganic content after pyrolysis and activation).

3.5 | Phenolic Compound Adsorption Tests

BBAs can prove valuable for a wide variety of applications [34, 60, 61], in this case for use as adsorbent or column packing material for separation applications [62, 63]. In this study, the produced BBAs are evaluated for their use in separating phenolic compounds (being a target extractive compound from various biomass streams) from NADES, which is not otherwise feasible through traditional distillation processes due to the intrinsic high boiling point of NADES solvents.

3.6 | Total Adsorption (q_e) of Phenolic Compound Mixtures From NADES

Adsorption tests in which ACs are suspended during 24 h in ChCl:Gly (Figure 5A) and ChCl:Ma (Figure 5B) NADES containing reference dosages of PC were used as a qualitative measure of their suitability as adsorber media. First, the effect of solvent environment is apparent in the overall lower adsorption capacity from ChCl:Ma (Figure 5B), which might be explained by stronger H-binding interactions between the acidic medium and phenolic compounds. Similar trends in the extraction yields for each individual PC remain observable, however.

It can be observed that in most BSG-based AC adsorbers, caffeic acid is adsorbed preferentially over the other three PC present, this stands in contrast with the reference AC which yields highest adsorption capacity for ferulic acid in both NADES media, but also higher coumaric acid adsorption from ChCl:Ma.

All four evaluated PC solutes have similar kinetic diameters, leading to the assumption that PSD of the ACs should not have a meaningful effect on adsorption of the individual species. Rather, influence of the total available surface area and potential chemical moieties present on the AC's surface should have a significant effect. Syringaldehyde has the least OH-substituted structure, followed by p-coumaric and ferulic acid. In comparison, caffeic acid can undergo H-bonding with both the acidic —COOH group, and the two meta- and para-substituted OH groups. From the extraction results, a clear preference can be observed toward higher-substituted adsorbates which have higher hydrogen-bonding capability.

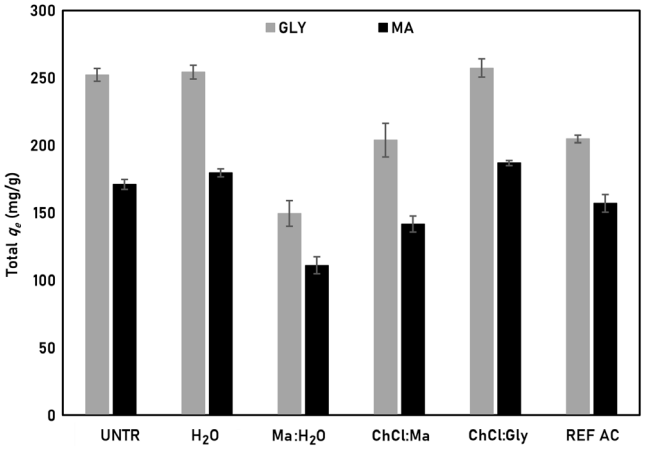

FIGURE 6 | Total sum of adsorption (q_e) of four phenolic compounds (CAF, SYR, COUM, FER) from 250 ppm stock solutions prepared in ChCl:Gly and ChCl:Ma NADES, using AC of: untreated BSG (UNTR); H_2O pretreated BSG (H_2O); aqueous malic acid pretreated BSG (Ma:H_2O); Ma:ChCl pretreated BSG (ChCl:Ma); Gly:ChCl NADES pretreated BSG (ChCl:Gly); Commercial reference AC (REF). Expressed as q_e (mg phenolic compound/g AC). (Results expressed as $\bar{x} \pm$ standard error (SE); $n = 2$).

Untreated, H_2O, and ChCl:Gly pretreated ACs share very similar adsorption results when comparing the sum of the equilibrium adsorptions (q_e) of all four phenolic compounds (Figure 6). For both tested media ChCl:Gly and ChCl:Ma, these three ACs represent an improved adsorption capacity of approximately 25% and 20%, respectively. The lower surface area of ChCl:Ma pretreated AC still yields a slightly higher adsorption capacity than the other acid pretreated sample Ma:H_2O and manages to retain similar adsorption capacity compared to the commercial reference material despite its high ash content and unfavorable surface area.

3.7 | Kinetic Adsorption of Phenolic Compound Mixtures From NADES

To demonstrate the application potential of the produced spent-biomass AC adsorbers, a kinetic experiment was set up in which stock solutions of NADES were prepared with mixtures of the four phenolic compounds. The competitive and reversible nature of adsorption allows to investigate if preferential adsorption takes place, based on the adsorbate structure. This is especially valuable in the context of using ACs as separating media for purification of extracts.

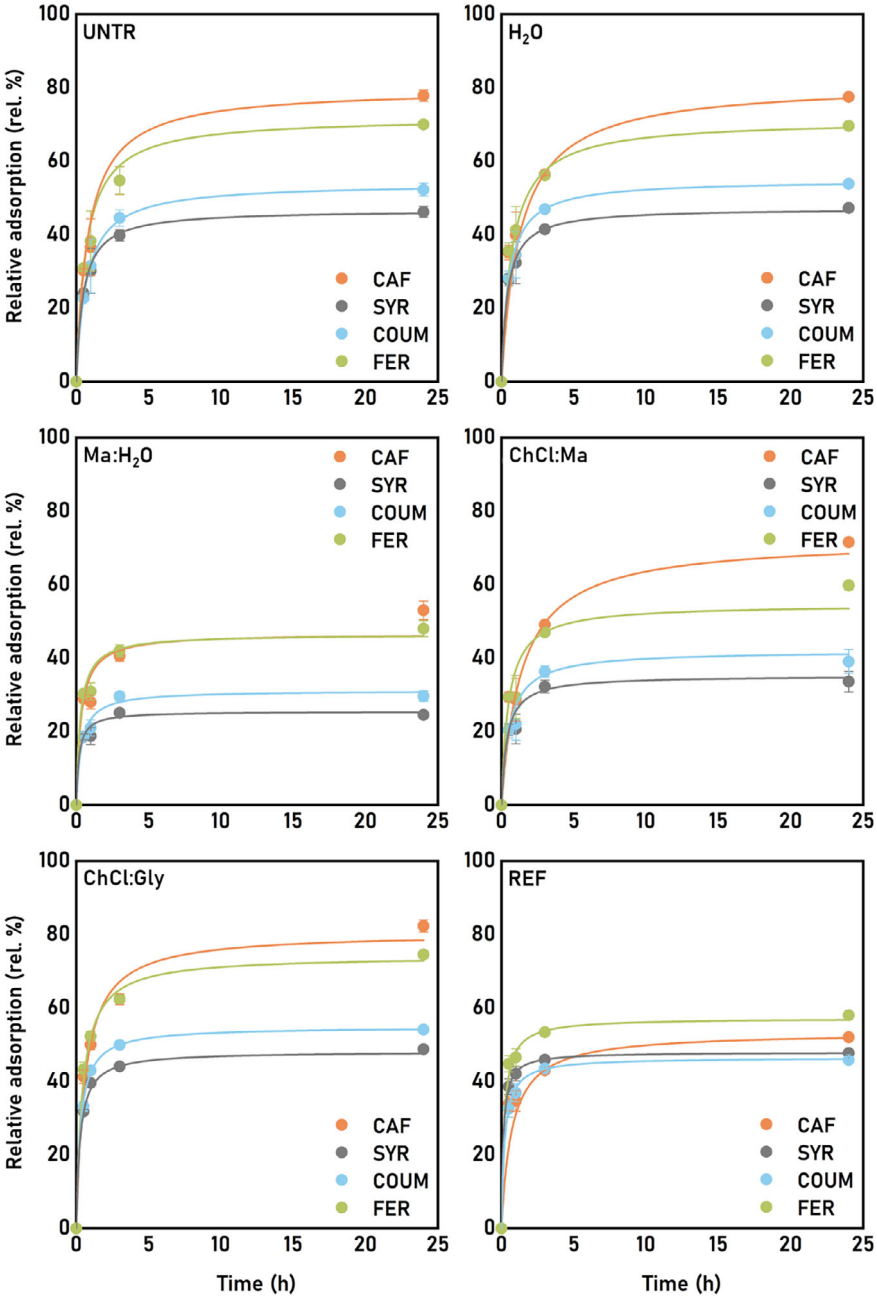

FIGURE 7 | Kinetics of adsorption of phenolic compounds from ChCl:Gly NADES solution (250 ppm of caffeic acid (CAF), syringaldehyde (SYR), p-coumaric acid (COUM), and ferulic acid (FER)) using AC of: untreated BSG (UNTR); H_2O pretreated BSG (H_2O); aqueous malic acid pretreated BSG (Ma:H_2O); Ma:ChCl pretreated BSG (ChCl:Ma); Gly:ChCl NADES pretreated BSG (ChCl:Gly); Commercial reference AC (REF). (Results expressed relative adsorption (rel.%), $\bar{x}$ ± standard error (SE); $n = 2$; solid lines represent the pseudosecond-order model fitting).

Sampling at different times of the adsorption experiment, it can be seen in Figures 7 and 8 how caffeic acid shows the slowest overall rate of adsorption, but some competitive effects can be seen in the case of Ma:H_2O pretreated AC, in which the adsorption of coumaric acid and syringaldehyde reaches a maximum around 3 h. Next, the total adsorbed amount of COU and SYR slightly reduced again until it reached 24 h adsorption time, in favor of a continued adsorption of caffeic acid and, to some extent, ferulic acid. In all instances of the BSG-based AC adsorbers, continuous adsorption changes can be observed for all PC in all media. This is in contrast with the adsorption on the reference AC, which reaches a steady-state condition around 3 h and preferentially adsorbs FER, as expected from previous adsorption experiments.

From Table 2, the pseudosecond-order rate constant (k_2) for all phenolic compounds is notably higher for the adsorption on Ma:H2O AC and (to a lesser degree) REF AC. These values exceed those observed for the ChCl:Ma and ChCl:Gly pretreated ACs. Elevated adsorption rate constants are typically associated with an increased mesopore content, as the more open pore structure of mesopores, typically found near the external surface of the carbon matrix, provides less restricted pathways for adsorbate diffusion into the internal pore network [64]. This interpretation is

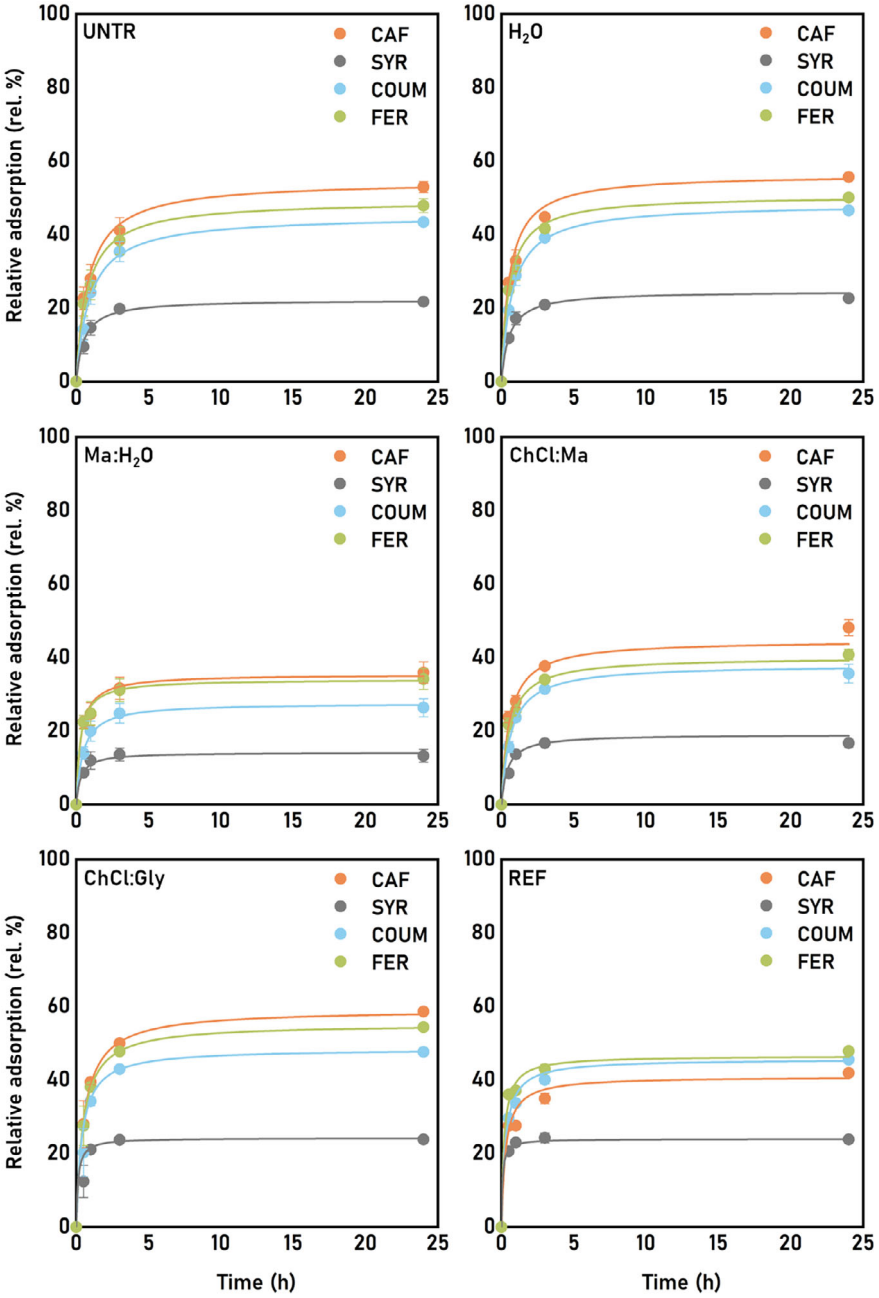

FIGURE 8 | Kinetics of adsorption of phenolic compounds from ChCl:Ma NADES solution (250 ppm of caffeic acid (CAF), syringaldehyde (SYR), p-coumaric acid (COUM), and ferulic acid (FER)) using AC of: untreated BSG (UNTR); H_2O pretreated BSG (H_2O); aqueous malic acid pretreated BSG (Ma:H_2O); Ma:ChCl pretreated BSG (ChCl:Ma); Gly:ChCl NADES pretreated BSG (ChCl:Gly); Commercial reference AC (REF). (Results expressed relative adsorption (rel.%), $\bar{x} \pm$ standard error (SE); $n = 2$; solid lines represent the pseudosecond-order model fitting).

TABLE 2 | Pseudosecond-order kinetic parameters (q_e: amount of adsorbate adsorbed at equilibrium; k_2: pseudosecond-order rate constant) of the adsorption of four model compounds from ChCl:Ma and Gly:ChCl NADES stock solutions (250 ppm of each; caffeic acid (CAF), syringaldehyde (SYR), p-coumaric acid (COUM), and ferulic acid (FER)) using AC of: untreated BSG (UNTR); H_2O pretreated BSG (H_2O); aqueous malic acid pretreated BSG (Ma:H_2O); Ma:ChCl pretreated BSG (ChCl:Ma); Gly:ChCl NADES pretreated BSG (ChCl:Gly); commercial reference AC (REF). (Results expressed as $\bar{x} \pm$ standard error (SE); $n = 2$).

	CAF		SYR		COUM		FER		TOTAL
	q_e	k_2	q_e	k_2	q_e	k_2	q_e	k_2	q_e
Adsorption from ChCl:Gly stock solution									
UNTR	79.7 ± 2.4	0.015 ± 0.001	46.7 ± 0.9	0.045 ± 0.003	54.0 ± 1.0	0.027 ± 0.002	71.9 ± 0.5	0.021 ± 0.001	252.3 ± 4.9
H_20	81.2 ± 2.4	0.010 ± 0.001	47.2 ± 0.8	0.052 ± 0.008	54.8 ± 0.5	0.037 ± 0.003	71.1 ± 1.6	0.019 ± 0.004	254.4 ± 5.3
Ma:H_20	46.6 ± 4.7	0.067 ± 0.028	25.4 ± 0.9	0.212 ± 0.057	31.1 ± 1.4	0.095 ± 0.025	46.4 ± 2.5	0.077 ± 0.020	149.6 ± 9.6
ChCl:Ma	72.3 ± 6.4	0.010 ± 0.004	35.2 ± 2.0	0.076 ± 0.022	41.9 ± 2.3	0.044 ± 0.012	54.5 ± 1.8	0.038 ± 0.010	203.9 ± 12.5
ChCl:Gly	80.4 ± 4.3	0.021 ± 0.005	48.1 ± 0.5	0.078 ± 0.010	54.8 ± 0.2	0.062 ± 0.003	74.1 ± 1.7	0.032 ± 0.005	257.3 ± 6.8
REF	53.4 ± 1.0	0.026 ± 0.003	47.9 ± 0.3	0.163 ± 0.024	46.5 ± 0.5	0.100 ± 0.015	57.1 ± 1.0	0.092 ± 0.026	204.9 ± 2.8
Adsorption from ChCl:Ma stock solution									
UNTR	54.6 ± 1.3	0.022 ± 0.004	22.2 ± 0.3	0.085 ± 0.018	45.1 ± 0.5	0.024 ± 0.003	49.2 ± 1.4	0.027 ± 0.005	171.1 ± 3.6
H_20	56.3 ± 1.1	0.033 ± 0.002	24.5 ± 0.4	0.076 ± 0.005	48.3 ± 0.5	0.028 ± 0.001	50.5 ± 1.0	0.037 ± 0.003	179.7 ± 2.9
Ma:H_20	35.4 ± 2.0	0.092 ± 0.026	14.1 ± 1.1	0.234 ± 0.086	27.6 ± 1.6	0.080 ± 0.021	34.0 ± 1.7	0.106 ± 0.028	111.1 ± 6.3
ChCl:Ma	44.6 ± 1.8	0.042 ± 0.012	19.0 ± 1.8	0.126 ± 0.054	38.0 ± 1.2	0.041 ± 0.006	40.0 ± 1.1	0.047 ± 0.010	141.6 ± 6.3
ChCl:Gly	59.1 ± 0.8	0.032 ± 0.003	24.2 ± 0.4	0.335 ± 0.131	48.4 ± 0.1	0.053 ± 0.003	55.2 ± 0.4	0.039 ± 0.003	186.9 ± 1.8
REF	40.9 ± 2.9	0.088 ± 0.031	24.0 ± 0.2	0.571 ± 0.094	45.7 ± 1.0	0.081 ± 0.007	46.6 ± 2.4	0.116 ± 0.041	157.1 ± 6.5

consistent with the PSD derived from N_2 and CO_2 physisorption measurements (Figure S2). Both Ma:H2O and REF ACs exhibit a moderately greater mesopore contribution compared to the other samples.

In contrast, when examining only the micropore region (<2 nm) of the PSD, the highest cumulative pore volume is observed for ChCl:Gly and H_2O AC's, whereas Ma:H_2O and ChCl:Ma AC's display a substantially lower microporosity. This distribution aligns with the expectation that micropores predominantly govern the adsorption of small organic molecules and thus are critical for achieving high equilibrium adsorption capacities (q_e).

Overall, it appears that the adsorption behavior can best be described by a pseudo-second-order adsorption model, which is based on the assumption that the rate-limiting step may be chemisorption. Mass transport does not likely appear to be the rate-limiting factor, due to the fact that k_2 values are higher for all adsorption experiments performed in ChCl:Ma, despite its higher viscosity than ChCl:Gly.

4 | Toward Ad- & Desorption of Phenolics From Real NADES Extracts Using BBAs

In an envisioned SPE setup, the AC should act as a catch-and-release medium for the phenolic antioxidants, while NADES solvent is separated off and recuperated. Preliminary experiments were conducted based on AC desorption experiments found in literature, in which ethanol was found to be a suitable desorption solvent for organic molecules such as dyes [65].

Due to the nature of the adsorption experiments being performed on small scale with only 10 mg of AC used in each sample, desorption experiments were limited to direct elution from the

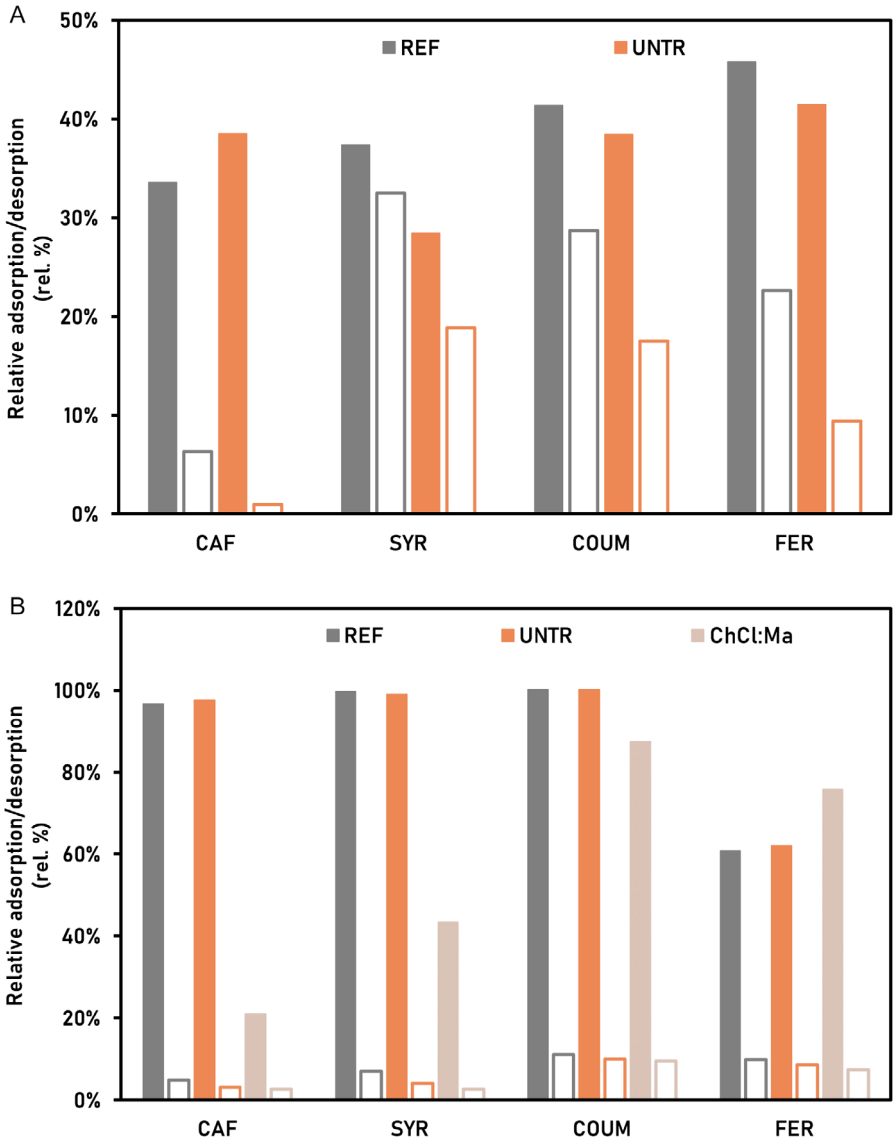

FIGURE 9 | Adsorption (full bars) and consecutive desorption using ethanol (open bars) of 4 phenolic compounds (PC; (CAF), syringaldehyde (SYR), p-coumaric acid (COUM), and ferulic acid (FER)) from: (A) stock solution of 250 ppm of each PC in ChCl:Gly NADES; (B) hydrothermal extract from BSG using ChCl:Ma NADES. Adsorptions were performed with commercial reference AC (REF), AC of untreated BSG (UNTR); AC of ChCl:Ma NADES pretreated BSG (ChCl:Ma).

syringe filters on which the ACs were collected. To facilitate homogenous elution, an automated syringe filter setup was used.

In Figure 9A, adsorption and consecutive desorption was first performed on a stock solution of 250 ppm of each PC in ChCl:Gly NADES. Relative to the initial PC concentration, approximately 6% of the initial CAF could be recovered after ad- and desorption with the commercial REF AC, while only 1% could be recovered with the UNTR BSG-based AC. These low recoveries once again confirm the strong preferential interactions between the highly substituted CAF and the ACs. For SYR, COUM, and FER, a substantially higher amount could be recovered in the ethanol phase, respectively 32%, 29%, and 23% from the REF AC, and 19%, 18%, and 9% from the UNTR AC.

Finally, recovering PCs from real NADES extracts (Figure 9B) is significantly more challenging due to the much lower starting concentrations in the extracts. Especially for HTE-ChCl:Gly extracts, the indirect concentration measurement through HPLC did not yield meaningful data, as the concentrations in the liquid NADES extracts were at most a few ppm.

For hydrothermal ChCl:Ma extracts, however, the recovered concentrations were high enough to quantify adsorption and desorption behavior, which are presented in Figure 9B. REF and UNTR ACs offered near-complete extraction of CAF, SYR, and COUM from the hydrothermal ChCl:Ma extract, even after only 1 h. Compared to the previous ads-/desorption experiment (Figure 9A), FER was now the least completely adsorbed, although this could be due to the high concentration of FER present in this particular extract. In contrast, ChCl:Ma pretreated AC performed significantly worse in adsorbing CAF, SYR, and COUM, yet adsorbed slightly more FER than the ChCl:Gly and UNTR ACs. For the subsequent desorption step, however, the low concentrations of PC adsorbed onto the ACs seemingly complicated the process, yielding at most 5%, 7%, 11%, and 10% recovery for CAF, SYR, COUM, and FER, respectively, with the use of the REF AC as adsorption medium. Both untreated (UNTR) and ChCl:Ma-pretreated (ChCl:Ma) AC's displayed lower PC recoveries.

Improving desorption efficiency is crucial to minimize the amount of organic solvent required for recovering PC from the BBAs, and the high cost associated with such a process. One reason for the low recovery of PC observed in this study, could be the relatively low initial PC concentrations in the extracts. Second, the lab-scale method (utilizing only a few mg of AC adsorber) to provide this proof-of-concept does not allow for ideal solvent-adsorbent contact time, limiting the possible mass transfer of PC from AC to the recovery solvent. Besides experimental limitations, further experimental work should be focused on facilitating mass transfer of PC from liquid to solid phase, for example, by decreasing the extract pH to suppress deprotonation, or by addition of small volumes of water as a poor solvent for the PC. Other, more advanced, solutions such as thermal or pH-based parametric pumping setups could be employed for concentrating the extract-rich phase, as well as providing additional control over the separation of targeted products [66, 67]. Given such optimisations, the proposed two-step extraction strategy—where NADES are first employed as highly effective extraction media, followed by a work-up and purification stage based on AC adsorption and classical organic solvent desorption—appears feasible for achieving both higher overall extraction yields and improved selectivity toward targeted compounds.

5 | Conclusions

A cascade valorization cycle for BSG residue was proposed. Herein, NADES-assisted extraction was stipulated as a pretreatment for biomass waste, in preparation for further valorization to AC. The effects of such pretreatments were shown to have strong consequences on the final characteristics of the obtained ACs.

The effects of the different pretreatment methods were highlighted through adsorption testing of targeted phenolic compounds. The adsorption capacity of ChCl:Gly pretreated AC showed on-par behavior to untreated and H_2O pretreated ACs with superior kinetic properties. As compared to a commercially available reference AC, the adsorber properties of ChCl:Ma and ChCl:Gly pretreated AC's were equal or higher than said reference.

On the other hand, acidic media such as Ma:H_2O and ChCl:Ma NADES showed a drastic reduction in carbonaceous residue after pyrolysis and CO_2 activation, inhibiting the formation of high-surface areas and capturing a relatively large amount of inorganic residue in the final AC's. The higher carbon burn-off, lower microporosity, and relatively high mesoporosity observed in these samples could indicate that these pretreated materials have a reduced recalcitrance and are thus more strongly converted toward larger and open pore structures, reducing their effectivity as BBAs. Additionally, more extensive carbon burn-off also has a negative ecological and economic impact of these materials, as less of the biomass carbon content is captured in the form of AC.

Finally, the preliminary desorption study performed in this section could provide an indication as to the feasibility of using ACs as separation media in NADES extracts. While recoveries of PC only reached approximately 10%, it must be mentioned that the desorption conditions were not optimized beyond the initial experiment, which leaves potential for improvement. Similarly, solvent usage for desorption was now approximately 150% of the initial volume of NADES extract, though given the low PC concentrations observed in these extracts, it can be reasonably assumed that a much larger quantity of extract could be adsorbed using the same amount of AC, therefore improving the solvent usage in the following desorption step.

With this study, a proof-of-concept is provided to show the feasibility of multiple additional use stages for traditional biomass food wastes, the changes in AC yields, chemical and physical properties, and ultimately their functioning as BBA, demonstrating the complexity of combining multiple process steps. While this study provides a solid groundwork for further work, it also must be highlighted that the nature of biomass remains deeply complex, and as such, these methods may not be implicitly transferable to any other biomass stream. Additionally, the feasibility of such a cascade valorization process is highly dependent on scalability of the processes. While upscaling falls outside the scope of this work, it is worth noting that the implementation of techniques, such as pyrolysis, adsorption and desorption, requires adaptation toward industrial scale-up. One such

adaptation would be the move from batch pyrolysis to a faster and more efficient continuous method in a screw-fed rotary kiln, as demonstrated on pilot scale by Lataf et al. [68] Another necessary scale-up change would be the switch toward preparative, AC-based columns for extract separation, which will allow for increased PC recovery due to the longer, tunable residence time on the separation column. Additionally, for economic and ecological considerations, pyrolysis and extraction/adsorption can be seen as highly complementary techniques in an integrated industrial process, due to their ability to recover thermal energy from the pyrolysis step for heating during the extraction phase.

Author Contributions

Dries Bleus: conceptualization (lead), methodology, investigation, formal analysis, data Curation, writing – original draft preparation. **Nahal Ghanemnia:** investigation, data curation, data analysis. **Wouter Marchal**: funding acquisition, conceptualization, supervision, writing – review & editing; **Dries Vandamme**: funding acquisition, conceptualization, resources, supervision, writing – review & editing.

Acknowledgments

This work was financially supported by BOF (BOF20OWB02) and EOS (G0H0522N). We would like to acknowledge Elsy Thijsen and Greet Cuyvers for support with ICP-OES and CHNS analysis and Philippe de Schryver for support with HPLC analysis.

Funding

This study was supported by BOF UHasselt (BOF20OWB02), Fonds Wetenschappelijk Onderzoek, EOS, the Excellence of Science (G0H0522N).

Conflicts of Interest

The authors declare no conflicts of interest.

Data Availability Statement

The data that support the findings of this study are available from the corresponding author upon reasonable request.

References

1. F. Barontini, M. Landi, L. D. Asaro, and E. Stefanelli, "Hydrothermal Carbonization of Brewer's Spent Grains : A Pathway for Brewery Waste Valorisation," *Chemical Engineering Transactions* 117 (2025): 163–168.

2. A. Nzihou, "Toward the Valorization of Waste and Biomass," *Waste and Biomass Valorization* 1 (2010): 3–7.

3. M. Alexandri, V. Kachrimanidou, H. Papapostolou, A. Papadaki, and N. Kopsahelis, "Sustainable Food Systems: The Case of Functional Compounds Towards the Development of Clean Label Food Products," *Foods* 11 (2022): 2796.

4. T. Raj and V. Singh, "Natural Deep Eutectic Solvents (NADES) Assisted Deconstruction of Oilcane Bagasse for High Lipid and Sugar Recovery," *Industrial Crops and Products* 210 (2024): 118127.

5. M. Jablonský, A. Škulcová, A. Malvis, and J. Šima, "Extraction of Value-Added Components From Food Industry Based and Agro-Forest Biowastes by Deep Eutectic Solvents," *Journal of Biotechnology* 282 (2018): 46–66.

6. A. Grudniewska and J. Popłoński, "Simple and Green Method for the Extraction of Xanthohumol From Spent Hops Using Deep Eutectic Solvents," *Separation and Purification Technology* 250 (2020): 117196.

7. J. C. López-Linares, V. Campillo, M. Coca, S. Lucas, and M. T. García-Cubero, "Microwave-Assisted Deep Eutectic Solvent Extraction of Phenolic Compounds From Brewer's Spent Grain," *Journal of Chemical Technology and Biotechnology* 96 (2020): 481–490.

8. N. Mirabella, V. Castellani, and S. Sala, "Current Options for the Valorization of Food Manufacturing Waste: A Review," *Journal of Cleaner Production* 65 (2014): 28–41.

9. K. Mishra, S. S. Siwal, S. C. Nayaka, Z. Guan, and V. K. Thakur, "Waste-to-Chemicals: Green Solutions for Bioeconomy Markets," *Science of the Total Environment* 887 (2023): 164006.

10. B. Mishra, Y. K. Mohanta, C. N. Reddy, et al., "Valorization of Agro-Industrial Biowaste to Biomaterials: An Innovative Circular Bioeconomy Approach," *Circular Economy* 2 (2023): 100050.

11. T. Keijer, V. Bakker, and J. C. Slootweg, "Circular Chemistry to Enable a Circular Economy," *Nature Chemistry* 11 (2019): 190–195.

12. A. Ncube, S. Mtetwa, M. Bukhari, G. Fiorentino, and R. Passaro, "Circular Economy and Green Chemistry: The Need for Radical Innovative Approaches in the Design for New Products," *Energies* 16 (2023): 1752.

13. N. Raina, S. Chuetor, D. Elalami, S. Tayibi, and A. Barakat, "Biomass Valorization for Bioenergy Production: Current Techniques, Challenges, and Pathways to Solutions for Sustainable Bioeconomy," *BioEnergy Research* 17 (2024): 1999–2028.

14. J. Rajesh Banu, Preethi, S. Kavitha, et al., "Lignocellulosic Biomass Based Biorefinery: A Successful Platform Towards Circular Bioeconomy," *Fuel* 302 (2021): 121086.

15. H. Ma, P. Fu, J. Zhao, et al., "Pretreatment of Wheat Straw Lignocelluloses by Deep Eutectic Solvent for Lignin Extraction," *Molecules* 27 (2022): 7955.

16. M. G. Morán-Aguilar, I. Costa-Trigo, M. Calderón-Santoyo, et al., "Enhancing the Biorefinery of Brewery Spent Grain by Deep Eutectic Solvent Pretreatment: Optimisation of Polysaccharide Enrichment Through a Response Surface Methodology," *Journal of Industrial and Engineering Chemistry* 145 (2025): 693–704.

17. Y. Wu, H. Ji, and X. Ji, "Biomass Pretreatment Using Biomass-Derived Organic Solvents Facilitates the Extraction of Lignin and Enzymatic Hydrolysis of Glucan," *Cellulose* 30 (2023): 2859–2872.

18. S. C. Rabelo, H. Carrere, R. Maciel Filho, and A. C. Costa, "Production of Bioethanol, Methane and Heat From Sugarcane Bagasse in a Biorefinery Concept," *Bioresource Technology* 102 (2011): 7887–7895.

19. M. Salgado-Ramos, S. Tabasso, E. Calcio Gaudino, A. Moreno, F. Mariatti, and G. Cravotto, "An Innovative, Green Cascade Protocol for Grape Stalk Valorization With Process Intensification Technologies," *Applied Sciences* 12 (2022): 7417.

20. V. Cheynier, "Phenolic Compounds: From Plants to Foods," *Phytochemistry Reviews* 11 (2012): 153–177.

21. N. Mahato, M. Sinha, K. Sharma, R. Koteswararao, and M. H. Cho, "Modern Extraction and Purification Techniques for Obtaining High Purity Food-Grade Bioactive Compounds and Value-Added Co-Products From Citrus Wastes," *Foods* 8 (2019): 523.

22. W. Routray and V. Orsat, "Microwave-Assisted Extraction of Flavonoids: A Review," *Food Bioprocess Technology* 5 (2012): 409–424.

23. D. Nkurunziza, A. Kumorkiewicz-Jamro, L. Yu, et al., "Differential Release of Biologically Active Cell-Wall-Bound Phenolics from Brewer's Spent Grain Using Conventional and Deep Eutectic Solvents," *ACS Sustainable Chemistry & Engineering* 13 (2025): 10794, https://doi.org/10.1021/acssuschemeng.5c00823.

24. P. P. Santiago, F. Andr, and R. S. D. Santiago-aguiar, "Valorization of Brewer's Spent Grain Through Ultrasound-Assisted Extraction of Phenolic Compounds Using Deep Eutectic Solvents," *ACS Omega* 10 (2025): 22603, https://doi.org/10.1021/acsomega.4c10526.

25. A. Zabaniotou, P. Kamaterou, V. Kachrimanidou, A. Vlysidis, and A. Koutinas, "Taking a Reflexive TRL3-4 Approach to Sustainable use of Sunflower Meal for the Transition From a Mono-Process Pathway to a Cascade Biorefinery in the Context of Circular Bioeconomy," *Journal of Cleaner Production* 172 (2018): 4119–4129.

26. D. Bleus, H. Blockx, E. Gesquiere, et al., "High-Temperature Hydrothermal Extraction of Phenolic Compounds From Brewer's Spent Grain and Malt Dust Biomass Using Natural Deep Eutectic Solvents," *Molecules* 29 (2024): 1983.

27. A. K. Singh, J. Y. Kim, and Y. S. Lee, "Phenolic Compounds in Active Packaging and Edible Films/Coatings:Natural Bioactive Molecules and Novel Packaging Ingredients," *Molecules* 27 (2022): 7513.

28. J. Dai and R. J. Mumper, "Plant Phenolics: Extraction, Analysis and Their Antioxidant and Anticancer Properties," *Molecules* 15 (2010): 7313–7352.

29. S. Anand, R. Sowbhagya, M. A. Ansari, et al., "Polyphenols and Their Nanoformulations: Protective Effects Against Human Diseases," *Life* 12 (2022): 1639, https://doi.org/10.3390/life12101639.

30. G. F. Cifuni, P. Caparra, E. Perri, C. Benincasa, G. Morone, and S. Claps, "Spray-Dried Phenolic Compounds From Olive Mill Waste Water as Animal Feed Supplement: Impact on the Aromatic Profile of Caciotta Cheese," *Molecules* 30 (2025): 3991.

31. M. S. B. da Cunha, C. M. T. S. Miguel, E. D. M. F. Lima, U. M. Pinto, C. V. Prudêncio, and S. D. Todorov, "Phenolic Compounds: From Traditional Uses to Innovative Applications and Everything in Between," *Molecular Nutrition & Food Research* 70 (2026): e70478, https://doi.org/10.1002/mnfr.70478.

32. S. Hong, X. Shen, Z. Xue, Z. Sun, and T.-Q. Yuan, "Structure–function Relationships of Deep Eutectic Solvents for Lignin Extraction and Chemical Transformation," *Green Chemistry* 22 (2020): 7219–7232.

33. E. Gomez-Delgado, D. Morales-Urrea, J. Alean, and A. López-Córdoba, "Activated Carbons from Brewers Spent Grain Improve Orange II Removal through Combined Adsorption and Enzymatic Oxidation," *Scientific Reports* 15, no. 1 (2025): 22487.

34. G. L. Sullivan, R. M. Prigmore, P. Knight, and A. R. Godfrey, "Activated Carbon Biochar From Municipal Waste as a Sorptive Agent for the Removal of Polyaromatic Hydrocarbons (PAHs), Phenols and Petroleum Based Compounds in Contaminated Liquids," *Journal of Environmental Management* 251 (2019): 109551.

35. D. Bhatia and A. K. Saroha, "Biochar Derived From Pyrolysis of Rice Straw as an Adsorbent for Removal of Phenol From Water," *Journal of Water Process Engineering* 59 (2024): 105003.

36. K. S. Fisher, and A. J. Vreugdenhil, "Adsorption of Chromium (VI) Using an Activated Carbon Derived from Petroleum Coke Feedstock," *International Journal of Molecular Sciences* 23 (2022): 16172.

37. P. L. Pasquet, Y. Abdou, M. Villain-Gambier, B. Ernst, and C. Bertagnolli, "Purification Process Coupling Membrane Filtration and Adsorption for Deep Eutectic Solvent (DES) Recycling After Lignin Extraction," *Bioresource Technology* 448 (2026): 134295.

38. Y. Patrice Didion, T. Gijsbert Tjalsma, Z. Su, M. Malankowska, and M. Pinelo, "What Is Next? the Greener Future of Solid Liquid Extraction of Biobased Compounds: Novel Techniques and Solvents Overpower Traditional Ones," *Separation and Purification Technology* 320 (2023): 124147, https://doi.org/10.1016/j.seppur.2023.124147.

39. J. G. Lynam, N. Kumar, and M. J. Wong, "Deep Eutectic Solvents' Ability to Solubilize Lignin, Cellulose, and Hemicellulose; Thermal Stability; and Density," *Bioresource Technology* 238 (2017): 684–689.

40. R. Lou and X. Zhang, "Evaluation of Pretreatment Effect on Lignin Extraction From Wheat Straw by Deep Eutectic Solvent," *Bioresource Technology* 344 (2022): 126174.

41. S. Hong, X.-J. Shen, B. Pang, et al., "In-Depth Interpretation of the Structural Changes of Lignin and Formation of Diketones During Acidic Deep Eutectic Solvent Pretreatment," *Green Chemistry* 22 (2020): 1851–1858.

42. H. Sun, X. Yuan, Z. Zhang, X. Su, and M. Shi, "Thermal Processing Effects on the Chemical Constituent and Antioxidant Activity of Okara Extracts Using Subcritical Water Extraction," *Journal of Chemistry* 2018 (2018): 6823789.

43. R. Diao, M. Sun, Y. Huang, and X. Zhu, "Synergistic Effect of Washing Pretreatment and Co-Pyrolysis on Physicochemical Property Evolution of Biochar Derived From Bio-Oil Distillation Residue and Walnut Shell," *Journal of Analytical and Applied Pyrolysis* 155 (2021): 105034.

44. D. O. Usino, T. Sar, P. Ylitervo, and T. Richards, "Effect of Acid Pretreatment on the Primary Products of Biomass Fast Pyrolysis," *Energies* 16 (2023): 2377.

45. B. Tiryaki, E. Yagmur, A. Banford, and Z. Aktas, "Comparison of Activated Carbon Produced From Natural Biomass and Equivalent Chemical Compositions," *Journal of Analytical and Applied Pyrolysis* 105 (2014): 276–283.

46. A. C. Lua and T. Yang, "Effect of Activation Temperature on the Textural and Chemical Properties of Potassium Hydroxide Activated Carbon Prepared From Pistachio-Nut Shell," *Journal of Colloid and Interface Science* 274 (2004): 594–601.

47. O. Ioannidou and A. Zabaniotou, "Agricultural Residues as Precursors for Activated Carbon Production-A Review," *Renewable and Sustainable Energy Reviews* 11 (2007): 1966–2005.

48. A. Korus, A. Szlęk, and A. Samson, "Physicochemical Properties of Biochars Prepared From Raw and Acetone-Extracted Pine Wood," *Fuel Processing Technology* 185 (2019): 106–116.

49. W. Wu, Y. Wang, and X. Hu, "Mass Transfer Driven Pore Engineering of Activated Carbon From the Activation of Biomass," *Green Chemistry* 28 (2026): 3486–3511.

50. A. Korus, J. P. Gutierrez, A. Szlęk, J. Jagiello, and A. Hornung, "Pore Development During CO2 and H2O Activation Associated With the Catalytic Role of Inherent Inorganics in Sewage Sludge Char and Its Performance During the Reforming of Volatiles," *Chemical Engineering Journal* 446 (2022): 137298.

51. C. W. Zhang, S. Q. Xia, and P. S. Ma, "Facile Pretreatment of Lignocellulosic Biomass Using Deep Eutectic Solvents," *Bioresource Technology* 219 (2016): 1–5.

52. Y. Sekiguchi and F. Shafizadeh, "The Effect of Inorganic Additives on the Formation, Composition, and Combustion of Cellulosic Char," *Journal of Applied Polymer Science* 29 (1984): 1267–1286.

53. S. D. Stefanidis, E. Heracleous, D. T. Patiaka, K. G. Kalogiannis, C. M. Michailof, and A. A. Lappas, "Optimization of Bio-Oil Yields by Demineralization of Low Quality Biomass," *Biomass and Bioenergy* 83 (2015): 105–115.

54. W. Vercruysse, C. L. Gomes, D. Bleus, et al., "Demineralization of Common Ivy-Derived Biomass and Biochar and Its Effect on the Resulting Activated Carbon Properties," *Separation and Purification Technology* 319 (2023): 124023.

55. R. C. Oglou, Y. Gokce, E. Yagmur, T. G. U. Ghobadi, and Z. Aktas, "Highly Stable Megalopolis Lignite Based N and S Self-Doped Hierarchically Porous Activated Carbons for High Performance Supercapacitors and Ash Content Effects on Performance," *Journal of Energy Storage* 46 (2022): 103817.

56. W. Spencer, D. Ibana, P. Singh, and A. N. Nikoloski, "Effect of Surface Area, Particle Size and Acid Washing on the Quality of Activated Carbon Derived from Lower Rank Coal by KOH Activation," *Sustainability* 16 (2024): 5876.

57. A. Selvarajoo and D. Oochit, "Effect of Pyrolysis Temperature on Product Yields of Palm Fibre and Its Biochar Characteristics," *Materials Science for Energy Technologies* 3 (2020): 575–583.

58. N. Ikenaga, H. Nakajima, H. Oda, and T. Suzuki, "CO_2 Gasification Behavior of Various Biomass Chars—Effect of Mineral Matters in Biomass Chars," *Science and Technology Reports of Kansai University* 51 (2009): 61–74.

59. Y. Huang, X. Yin, C. Wu, et al., "Effects of Metal Catalysts on CO_2 Gasification Reactivity of Biomass Char," *Biotechnology Advances* 27 (2009): 568–572.

60. O. C. Iheanacho, J. T. Nwabanne, C. C. Obi, and C. E. Onu, "Packed Bed Column Adsorption of Phenol Onto Corn Cob Activated Carbon: Linear and Nonlinear Kinetics Modeling," *South African Journal of Chemical Engineering* 36 (2021): 80–93.

61. O. Adam, "Removal of Resorcinol From Aqueous Solution by Activated Carbon: Isotherms, Thermodynamics and Kinetics," *American Chemical Science Journal* 16 (2016): 1–13.

62. M. Najafi, Z. A. Abousadi, B. Honarvar, and S. A. Sajadian, "Separation of Hydrocarbons From Activated Carbon as a Porous Substance in a Glycol Regeneration Process Using Supercritical Carbon Dioxide," *Scientific Reports* 12 (2022): 1–18.

63. X. Ge, Z. Wu, M. Manzoli, Z. Wu, and G. Cravotto, "Feasibility and the Mechanism of Desorption of Phenolic Compounds From Activated Carbons," *Industrial & Engineering Chemistry Research* 59 (2020): 12223–12231.

64. G. Wang, X. Yong, L. Luo, S. Yan, J. W. C. Wong, and J. Zhou, "Structure-Performance Correlation of High Surface Area and Hierarchical Porous Biochars as Chloramphenicol Adsorbents," *Separation and Purification Technology* 296 (2022): 121374.

65. S. Bourahla, F. Nemchi, H. Belayachi, A. Belayachi, C. Harrats, and M. Belhakem, "Removal of the AO7 Dye by Adsorption on Activated Carbon Based on Grape Marc: Equilibrium, Regeneration, and FTIR Spectroscopy," *Journal of the Iranian Chemical Society* 20 (2023): 669–681.

66. M. D. L. Soto, A. Moure, H. Domínguez, and J. C. Parajó, "Recovery, Concentration and Purification of Phenolic Compounds by Adsorption: A Review," *Journal of Food Engineering* 105 (2011): 1–27.

67. M. Otero, M. Zabkova, and A. E. Rodrigues, "Phenolic Wastewaters Purification by Thermal Parametric Pumping: Modeling and Pilot-Scale Experiments," *Water Research* 39 (2005): 3467–3478.

68. A. Lataf, R. Carleer, J. Yperman, et al., "The Screening of Various Biochars for Cd2+ Removal at Relevant Soil pH," *Waste Management* 168 (2023): 376–385.

Supporting Information

Additional supporting information can be found online in the Supporting Information section.